Common Variants in the Complement Factor H Gene Confer Genetic Susceptibility to Central Serous Chorioretinopathy

Akiko Miki, MD,[1] Naoshi Kondo, MD, PhD,[1,2] Suiho Yanagisawa, MD,[1] Hiroaki Bessho, MD, PhD,[1] Shigeru Honda, MD, PhD,[1] Akira Negi, MD, PhD[1]

Purpose: To investigate whether complement factor H (*CFH*) gene DNA variants are associated with central serous chorioretinopathy (CSCR).

Design: Cross-sectional study.

Participants: A case-control group of 140 CSCR subjects and 2 different control groups: 934 population-based controls and 335 hospital-based controls.

Methods: Five single-nucleotide polymorphisms (SNPs) in *CFH* (rs3753394, rs800292, rs2284664, rs1329428, and rs106548) were evaluated for association with CSCR in 2 separate association analyses comparing CSCR subjects with 2 different control groups. Genotyping was performed using TaqMan technology (Applied Biosystems, Foster City, CA).

Main Outcome Measures: Allele and haplotype frequencies of the 5 variants in the *CFH* region.

Results: Highly statistically significant associations with CSCR were found for the 5 SNPs. The strongest association was observed with rs1329428 (allelic $P = 6.44 \times 10^{-6}$; odds ratio, 1.79; 95% confidence interval [CI], 1.39–2.31, cases vs. population-based controls), which accounted for 35.5% of the population-attributable fraction for CSCR. Consistent with the analysis, rs1329428 showed the strongest disease association (allelic $P = 1.00 \times 10^{-5}$; odds ratio, 1.89; 95% CI, 1.42–2.50) in comparing cases with hospital-based controls. The second most strongly associated SNP, rs1065489, was correlated highly with the most strongly associated SNP, rs1329428 ($r^2 = 0.77$), and their effects could not be distinguished statistically from each other. A conditional logistic regression analysis revealed that the 2 highly correlated SNPs, rs1329428 and rs1065489, account for the association signals detected at the *CFH* locus.

Conclusions: We identified a novel association between CSCR and common *CFH* polymorphisms. Our findings support the involvement of CFH in the pathogenesis of CSCR; exploration of the role of *CFH* could yield important insights into the biological mechanisms underlying CSCR. Our identification of common *CFH* variants as susceptibility elements for CSCR will open new avenues for research, leading to a better understanding of CSCR pathogenesis and ultimately to the development of improved therapeutic approaches. *Ophthalmology 2014;121:1067-1072 © 2014 by the American Academy of Ophthalmology.*

Central serous chorioretinopathy (CSCR) is characterized by localized detachment of the neurosensory retina at the macula, predominantly in middle-aged males.[1,2] Although retinal detachment in CSCR often resolves spontaneously, 30% to 50% of cases are chronic, recurrent, or both, causing damage to foveal photoreceptors.[2]

Abnormalities of choroidal circulation are thought to play a pivotal role in the pathogenesis of CSCR; distinct choroidal abnormalities, including choroidal vascular hyperpermeability, filling delay, and venous congestion, can be visualized by indocyanine green angiography.[1,2] These abnormalities may cause decompensation of the overlying retinal pigment epithelium, leading to focal or diffuse breakdown of the outer retinal barrier and neuroretinal detachment. However, the primary trigger for these choroidal abnormalities and the precise sequence of events involved in CSCR remain elusive.

The familial clustering of CSCR[1] suggests that there are genetic susceptibility loci for the disease; however, there has been no genetic survey for CSCR susceptibility loci, and the genetic basis of CSCR, if any, currently is unknown. In this study, we focused on the complement factor H (*CFH*) gene as a candidate susceptibility gene for CSCR because the protein binds to adrenomedullin,[3,4] a calcitonin family peptide that is a strong vasodilator in the choroid, thereby affecting choroidal hemodynamics.[5] Adrenomedullin previously was proposed to be implicated in the cause of CSCR.[6] Thus, we investigated the possible role of *CFH* in CSCR in a genetic association study, genotyping 5 singlenucleotide polymorphisms (SNPs) spanning the *CFH* locus in 140 CSCR cases and 934 population-based and 335 hospital-based controls.

Methods

Study Participants

The study protocol was approved by the institutional review board at Kobe University Graduate School of Medicine and was performed in accordance with the Declaration of Helsinki. Written

ISSN 0161-6420/14/$ - see front matter
http://dx.doi.org/10.1016/j.ophtha.2013.11.020

informed consent was obtained from all subjects before participation in this study. All case subjects were Japanese individuals recruited from the Department of Ophthalmology at Kobe University Hospital in Kobe, Japan. We used 2 different control groups: (1) genome-wide screening data from BioBank Japan control samples (control-JSNP) from 934 healthy volunteers and serving as a general population control, as previously described[7,8]; and (2) 335 control subjects previously recruited from the Department of Ophthalmology at Kobe University Hospital in Kobe, Japan (control-Kobe). The genotype data for the control-JSNP samples are available at the JSNP database (available at: http://snp.ims.u-tokyo.ac.jp/; accessed September 2, 2012). The database provides genotype data for 515 286 SNPs in autosomal chromosomes of the 934 Japanese volunteers without individual genotype data. In contrast, we had complete individual genotype data for the 5 *CFH* variants in the control-Kobe samples, which enabled us to perform a conditional logistic regression and haplotype analysis. A portion of the control-Kobe subjects participated in previous studies; the phenotyping criteria previously were described completely.[9,10] None of the control-Kobe subjects had a history of CSCR.

The demographic details of the study population are shown in Table 1. All CSCR subjects underwent a comprehensive ophthalmic examination, including visual acuity measurement, slit-lamp biomicroscopy of the fundi, color fundus photographs, optical coherence tomography, fluorescein angiography, and indocyanine green angiography. All our cases had subretinal fluid at the central macula visible on funduscopy and optical coherence tomography, and fluorescein angiography showed dye leakage from the retinal pigment epithelium. Patients receiving exogenous corticosteroids or patients showing evidence of uveitis, ocular trauma, retinal vascular diseases, choroidal neovascularization, or other diseases that can cause macular exudation, such as age-related macular degeneration (AMD), polypoidal choroidal vasculopathy, pathologic myopia, and angioid streaks, were excluded.

Genotyping

Genomic DNA was extracted from peripheral blood by standard methods. For cases and the control-Kobe subjects, genotyping was performed using TaqMan SNP Genotyping Assays (Applied Biosystems, Foster City, CA) on a StepOnePlus Real-Time PCR System (Applied Biosystems) in accordance with the manufacturer's recommendations. The control-JSNP samples were genotyped using the Illumina HumanHap550 BeadChip (available at: http://snp.ims.u-tokyo.ac.jp/; accessed September 2, 2012).

Single Nucleotide Polymorphism Selection

We searched for SNPs in the *CFH* region that were genotyped in the 934 BioBank Japan samples using the JSNP database (available at: http://snp.ims.u-tokyo.ac.jp/; accessed September 2, 2012). Five *CFH* SNPs (rs3753394, rs800292, rs2284664, rs1329428, and rs1065489) were found in the JSNP database, and all were selected for genotyping in the cases and control-Kobe subjects.

Table 1. Characteristics of the Study Population

	Central Serous Chorioretinopathy Group	Control Japanese Single Nucleotide Polymorphism Group	Control Kobe Group
No. of subjects	140	934	335
Sex (male/female)	118/22	684/250	183/152
Mean age ± SD (yrs)	49±10.3	52±15.0	71±7.2
Age range (yrs)	27–81	NA	50–95

NA = not available; SD = standard deviation.
Demographic information for the Control Japanese Single Nucleotide Polymorphism group has been reported previously.[7]

Statistical Analysis

Allelic associations were evaluated for each SNP by chi-square tests on 2×2 contingency tables using PLINK software version 1.07 (available at: http://pngu.mgh.harvard.edu/purcell/plink/; accessed May 1, 2013). All odds ratios (ORs) and corresponding 95% confidence intervals (CIs) were reported with respect to minor alleles in the controls. For the allelic association tests, we applied a Bonferroni correction for multiple testing, where nominal P values were multiplied by 5 (the number of SNPs tested for association). Deviations from Hardy-Weinberg equilibrium were analyzed by the exact test implemented in PLINK.[11] The pattern of risk associated with SNPs was examined by 3 additional association tests under 3 inheritance models (additive, dominant, and recessive) performed by logistic regression and implemented in SNPStats (available at: http://bioinfo.iconcologia.net/SNPStats; accessed May 2, 2013). The Akaike information criterion was used to compare these genetic models. The population-attributable fraction was calculated as previously described.[12] Possible functional consequences of SNPs on protein sequence, transcriptional regulation, RNA splicing, and miRNA binding were investigated using the SNPinfo database (available at: http://snpinfo.niehs.nih.gov/; accessed May 2, 2013) and the programs Polyphen (available at: http://genetics.bwh.harvard.edu/pph/; accessed May 2, 2013) and FASTSNP (available at: http://fastsnp.ibms.sinica.edu.tw/pages/input_Candidate-GeneSearch.jsp; accessed May 2, 2013). Haploview software (available at: http://www.broadinstitute.org/scientific-community/science/programs/medical-and-population-genetics/haploview/haploview; accessed May 2, 2013) was used to assess linkage disequilibrium (LD) patterns and haplotype association statistics. Haplotype blocks were determined using a solid spine of the LD algorithm with a minimum D′ value of 0.8. To correct for multiple testing in the haplotype association analysis, 10 000 permutations were run using this software. An omnibus (or global) test of the haplotype association and OR and 95% CI calculation for haplotype-specific risks were performed with PLINK.

Results

Five SNPs (rs3753394, rs800292, rs2284664, rs1329428, and rs1065489) initially were tested for associations with CSCR in 140 case and 934 control-JSNP samples, none of which deviated significantly from Hardy-Weinberg equilibrium ($P > 0.05$). All 5 SNPs were found to be associated significantly with CSCR after Bonferroni correction for multiple testing (Table 2). rs1329428 Had the strongest association (allelic $P = 6.44\times10^{-6}$), followed by rs1065489 (allelic $P = 6.56\times10^{-5}$), rs800292 (allelic $P = 6.75\times10^{-5}$), rs2284664 (allelic $P = 7.84\times10^{-4}$), and rs3753394 (allelic $P = 0.0017$). We performed additional analysis to assess the pattern of risk associated with the most strongly associated SNP, rs1329428. Our results suggest that an additive genetic model—with an OR of 1.82 (95% CI, 1.39–2.33)—would be the most parsimonious model (Akaike information criterion, 814.9, 823.1, and 820.4 for additive, dominant, and recessive models, respectively). The population-attributable fraction of rs1329428 for CSCR was 35.5% in our study cohort.

Because the JSNP database (available at: http://snp.ims.u-tokyo.ac.jp/; accessed September 2, 2012) does not provide individual genotype data for the control-JSNP samples, it was not possible to perform haplotype analysis or conditional logistic

Table 2. Results of Single-Marker Association Tests

Single Nucleotide Polymorphism (Location)	Position in NCBI Build 36.3	Alleles*	Minor Allele Frequency		Association Results		
			Cases (n = 140)	*Control-Japanese Single Nucleotide Polymorphism Group† (n = 934)*	*Nominal Allelic P Value*	*Allelic Odds Ratio (95% Confidence Interval)*	*Bonferroni-Corrected P Value‡*
rs3753394 (promoter)	47111271 bp	T/C	0.586	0.485	0.0017	1.50 (1.16–1.94)	0.0085
rs800292 (exon 2; I62V)	47132587 bp	G/A	0.529	0.403	6.75×10^{-5}	1.66 (1.29–2.14)	3.38×10^{-4}
rs2284664 (intron 15)	47192879 bp	C/T	0.496	0.391	7.84×10^{-4}	1.54 (1.19–1.98)	0.0039
rs1329428 (intron 15)	47193164 bp	C/T	0.593	0.449	6.44×10^{-6}	1.79 (1.39–2.31)	3.22×10^{-5}
rs1065489 (exon 18; D936E)	47200128 bp	G/T	0.350	0.478	6.56×10^{-5}	0.59 (0.45–0.77)	3.28×10^{-4}

*Major/minor alleles.
†Data for BioBank Japan control samples were obtained from the Japanese Single Nucleotide Polymorphism database (http://snp.ims.u-tokyo.ac.jp/).
‡Bonferroni-corrected *P* values were generated by multiplying the nominal allelic *P* values by 5.

regression. We therefore evaluated these genetic associations by comparing the CSCR subjects with an additional panel of 335 control-Kobe samples. This test enabled us to carry out haplotype and conditional analyses because we had complete individual genotype data for the 5 CSCR-associated SNPs (rs3753394, rs800292, rs2284664, rs1329428, and rs1065489) in the control-Kobe samples. First, we individually analyzed each of the 5 SNPs. Minor allele frequencies of the 5 SNPs in the control-Kobe samples were almost identical to those in the BioBank Japan samples (Tables 2 and 3), and all were in Hardy-Weinberg equilibrium ($P > 0.05$). This association analysis also demonstrated significant evidence of associations between these 5 SNPs and CSCR (Table 3). Consistent with the previous analysis, rs1329428 showed the strongest disease association (allelic $P = 1.00\times10^{-5}$; OR, 1.89; 95% CI, 1.42–2.50; Table 3).

Next, we constructed a pairwise LD structure with the 5 SNPs (Fig 1). Given that the 5 CSCR-associated SNPs are correlated substantially with each other ($r^2 \geq 0.38$; Fig 1), we tested the independence of the evidence for the multiple associations by performing a conditional logistic regression analysis of these 5 SNPs. After controlling for the genetic effect of rs1329428, the association evidence for the remaining 4 SNPs was no longer significant (smallest $P_{conditional} = 0.477$). In contrast, rs1329428 maintained a significant association when any other SNPs (except rs1065489) were used to seed the model. The 2 SNPs, rs1329428 and rs1065489, were correlated highly with each other ($r^2 = 0.77$), and their genetic effects could not be separated statistically (fitting one in the conditional logistic regression model rendered the other redundant). Similarly, conditional on rs1065489, no other SNP showed significant evidence of association (smallest $P_{conditional} = 0.174$), whereas rs1065489 remained significant after conditioning on any SNPs other than rs1329428.

Finally, we performed haplotype analysis of the *CFH* region. As shown in Figure 1, 2 haplotype blocks were defined, and association with the disease was found in both blocks, as demonstrated by the significant omnibus results (omnibus $P = 0.00276$ and $P = 2.27\times10^{-4}$ for blocks 1 and 2, respectively; Table 4). Two haplotypes in each block were found to be associated significantly with CSCR after correction for multiple testing (permutation $P < 0.05$; Table 4). The haplotype CCT in block 2 was associated most strongly with CSCR, appearing on 35.0% of CSCR chromosomes in comparison with 49.9% of control chromosomes ($P = 2.78\times10^{-5}$). This haplotype was described completely by the allele T at rs1065489, but its haplotypic *P* value did not increase with statistical significance compared with the single-allele analysis of rs1065489 (Table 3). No haplotype showed stronger association than the single-allele analysis.

Discussion

No genetic variants associated with the risk of CSCR have yet been reported. We tested 5 common *CFH* variants (rs3753394, rs800292, rs2284664, rs1329428, and rs1065489) for associations with CSCR and found statistically significant evidence for associations with each of these 5 variants. The strongest association was observed with rs1329428 ($P = 6.44\times10^{-6}$), which accounted for 35.5% of the population-attributable fraction of CSCR. The second most strongly associated SNP, rs1065489, was correlated highly with the most strongly associated SNP, rs1329428 ($r^2 = 0.77$), and their effects could not be statistically distinguished from each other. A conditional logistic

Table 3. Single-Marker Association Analysis Using the Alternate Control Group

Single Nucleotide Polymorphism	Alleles*	Minor Allele Frequency		Association Results	
		Cases (n = 140)	*Control Kobe Group† (n = 335)*	*Allelic P Value*	*Allelic Odds Ratio (95% Confidence Interval)*
rs3753394	T/C	0.586	0.487	0.0053	1.49 (1.13–1.98)
rs800292	G/A	0.529	0.406	5.22×10^{-4}	1.64 (1.24–2.17)
rs2284664	C/T	0.496	0.366	1.81×10^{-4}	1.71 (1.29–2.27)
rs1329428	C/T	0.593	0.436	1.00×10^{-5}	1.89 (1.42–2.50)
rs1065489	G/T	0.35	0.499	2.78×10^{-5}	0.54 (0.41–0.72)

*Major/minor alleles.
†Originally recruited controls from the Department of Ophthalmology at Kobe University Hospital in Kobe, Japan.

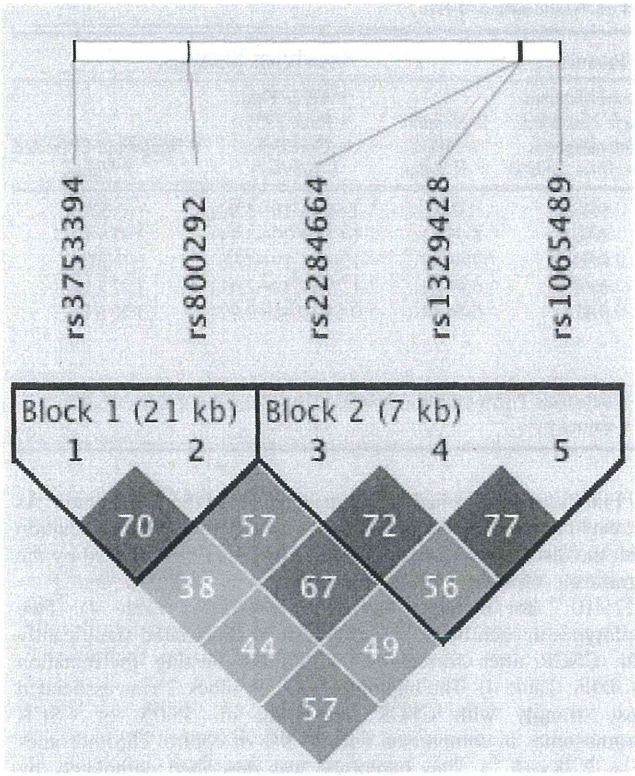

Figure 1. Linkage disequilibrium (LD) structure of the complement factor H gene. Linkage disequilibrium was measured using data from cases and the control-Kobe samples in this study. The haplotype blocks were determined using a solid spine of the LD algorithm with a minimum D′ value of 0.8. Each box provides estimated statistics of the coefficient of determination (r^2), with darker shades representing stronger LD.

regression analysis revealed that the multiple associations within the *CFH* locus are not independent because of the high LD across the region, and the 2 highly correlated SNPs, rs1329428 and rs1065489, account for the association signals detected at the locus.

CFH is a critical negative regulator of the alternative pathway of the complement system[13]; *CFH* inhibits C3 convertases either by binding to C3b and inhibiting its interaction with factor B or by promoting the decay of existing C3bBb complexes. *CFH* is also an essential cofactor for the factor I–mediated proteolytic inactivation of C3b. It is noteworthy that *CFH* also binds and interacts with adrenomedullin,[3,4] a member of the calcitonin peptide family that has been shown to induce vasodilation of vascular beds in the choroid and to affect choroidal blood flow.[5] Furthermore, adrenomedullin is known to increase microvascular permeability.[6] How the *CFH* variants are a source of genetic risk for CSCR is unclear, but these hemodynamic activities of adrenomedullin suggest a biological mechanism underlying the association of *CFH* variants and CSCR, given that vasodilation, altered blood flow, and hyperpermeability in the choroidal vessels are key features of CSCR.[1,2]

The *CFH* region on chromosome 1q32 is one of the best-established susceptibility loci for AMD.[14–19] All 5 SNPs tested here also are associated with AMD but in the opposite directions to their associations with CSCR.[14–19] The minor alleles of rs3753394, rs800292, rs2284664, and rs1329428 are protective for AMD but are risk alleles for CSCR. In contrast, the minor allele of rs1065489 confers risk of AMD, but was protective for CSCR. Age-related macular degeneration is a neurodegenerative disease of the macula involving the neural retina, retinal pigment epithelium, and choroid.[20] Association of opposite alleles of the same susceptibility variant with a series of autoimmune diseases frequently has been reported. For example, opposing alleles of the same variant confer risk of multiple autoimmune diseases, such as multiple sclerosis, rheumatoid arthritis, psoriatic arthritis, ankylosing spondylitis, Crohn's disease, and type 1 dia-betes.[21–24] Polymorphisms or mutations in *CFH* are associated with various diseases, including membranoproliferative glomerulonephritis type II or dense deposit disease, immunoglobulin A nephropathy, atypical hemolytic uremic syndrome, as well as AMD.[4,25,26] The same variation in *CFH* has been found to exert an opposite effect; certain alleles are associated with disease in atypical hemolytic uremic syndrome but are protective against immunoglobulin A nephropathy and AMD.[25] These findings suggest that phenotypic expression of variant alleles is affected differentially by environmental factors and interactions with multiple other genetic loci.

Table 4. Association of Complement Factor H Haplotype Blocks with Central Serous Chorioretinopathy

Block	Haplotype	Frequency		P Value*	Odds Ratio (95% Confidence Interval)	Omnibus P Value†
		Cases	*Controls*			
1: rs3753394|rs800292	TG	0.410	0.507	0.0064	0.69 (0.53–0.91)	0.00276
	CA	0.525	0.40	4.0×10^{-4}	1.63 (1.23–2.16)	
	CG	0.061	0.087	0.181	0.68 (0.39–1.19)	
2: rs2284664|rs1329428|rs1065489	CCT	0.350	0.499	2.78×10^{-5}	0.55 (0.41–0.73)	2.27×10^{-4}
	TTG	0.496	0.366	2.0×10^{-4}	1.66 (1.26–2.19)	
	CTG	0.096	0.070	0.168	1.41 (0.86–2.32)	
	CCG	0.057	0.066	0.622	0.86 (0.48–1.55)	

The association of haplotype CA and TG in block 1 (permutation $P = 0.0029$ and $P = 0.0379$, respectively) and haplotype CCT and TTG in block 2 (permutation $P = 2.0\times10^{-4}$ and $P = 0.0017$, respectively) remained statistically significant after correction for multiple testing.
*P values were calculated by the chi-square test on haplotype counts (1 degree of freedom).
†Omnibus P values were calculated using PLINK software (2 degrees of freedom for block 1; 3 degrees of freedom for block 2).

Our study is not sufficiently comprehensive to warrant screening for variants in the *CFH* region. According to data from the HapMap Project for the Japanese population, there are 34 SNPs with minor allele frequencies of more than 0.1 across the *CFH* region, but we genotyped only 5 SNPs. Of the 2 variants (rs1329428 and rs1065428) that primarily drive the association detected at the *CFH* locus in this study, rs1329428 maps to intron 15 and rs1065489 is a non-synonymous SNP in exon 18. Bioinformatics did not reveal any putative functional consequences of the intronic SNP rs1329428. rs1065489 Causes a Glu936Asp substitution, but it was predicted to be benign by the Polyphen algorithm. Thus, the functional basis of these associations currently is unclear. Comprehensive analysis of the *CFH* region with denser SNP panels will allow refinement of the risk interval and will provide a more detailed picture of the genetic susceptibility conferred by sequence variants in this region.

In summary, we identified a novel association between common *CFH* variants and CSCR. Our findings support the involvement of *CFH* in the pathogenesis of CSCR, and exploration of this mechanism could yield important insights into the biological mechanisms underlying CSCR. This is the first report stating that genomic variations in *CFH* confer genetic susceptibility to CSCR, and validation of our results in other populations will provide further convincing evidence for the genetic association.

Acknowledgments. The authors thank Shin-ichi Kuno, PhD, for providing the extensive statistical assistance.

References

1. Gemenetzi M, De Salvo G, Lotery AJ. Central serous chorioretinopathy: an update on pathogenesis and treatment. Eye (Lond) 2010;24:1743–56.
2. Klais CM, Ober MD, Ciardella AP, Yanuzzi LA. Central serous chorioretinopathy. In: Ryan SJ ed-in-chief, Hinton DR, Schachat AP, Wilkinson P, eds. Retina. vol. 2. 4th ed. Philadelphia: Elsevier/Mosby; 2006:1135–61.
3. Pio R, Martinez A, Unsworth EJ, et al. Complement factor H is a serum-binding protein for adrenomedullin, and the resulting complex modulates the bioactivities of both partners. J Biol Chem 2001;276:12292–300.
4. Boon CJ, van de Kar NC, Klevering BJ, et al. The spectrum of phenotypes caused by variants in the *CFH* gene. Mol Immunol 2009;46:1573–94.
5. Dorner GT, Garhöfer G, Huemer KH, et al. Effects of adrenomedullin on ocular hemodynamic parameters in the choroid and the ophthalmic artery. Invest Ophthalmol Vis Sci 2003;44:3947–51.
6. Udono-Fujimori R, Udono T, Totsune K, et al. Adrenomedullin in the eye. Regul Pept 2003;112:95–101.
7. Asano K, Matsushita T, Umeno J, et al. A genome-wide association study identifies three new susceptibility loci for ulcerative colitis in the Japanese population. Nat Genet 2009;41:1325–9.
8. Nakanishi H, Yamada R, Gotoh N, et al. A genome-wide association analysis identified a novel susceptible locus for pathological myopia at 11q24.1. PLoS Genet [serial online] 2009;5:e1000660. Available at: http://www.plosgenetics.org/article/info%3Adoi%2F10.1371%2Fjournal.pgen.1000660. Accessed October 30, 2013.
9. Kondo N, Honda S, Kuno S, Negi A. Coding variant I62V in the complement factor H gene is strongly associated with polypoidal choroidal vasculopathy. Ophthalmology 2009;116:304–10.
10. Kondo N, Honda S, Kuno S, Negi A. Role of *RDBP* and *SKIV2L* variants in the major histocompatibility complex class III region in polypoidal choroidal vasculopathy etiology. Ophthalmology 2009;116:1502–9.
11. Wigginton JE, Cutler DJ, Abecasis GR. A note on exact tests of Hardy-Weinberg equilibrium. Am J Hum Genet 2005;76:887–93.
12. van der Zanden LF, van Rooij IA, Feitz WF, et al. Common variants in *DGKK* are strongly associated with risk of hypospadias. Nat Genet 2011;43:48–50.
13. Ricklin D, Hajishengallis G, Yang K, Lambris JD. Complement: a key system for immune surveillance and homeostasis. Nat Immunol 2010;11:785–97.
14. Klein RJ, Zeiss C, Chew EY, et al. Complement factor H polymorphism in age-related macular degeneration. Science 2005;308:385–9.
15. Edwards AO, Ritter R III, Abel KJ, et al. Complement factor H polymorphism and age-related macular degeneration. Science 2005;308:421–4.
16. Haines JL, Hauser MA, Schmidt S, et al. Complement factor H variant increases the risk of age-related macular degeneration. Science 2005;308:419–21.
17. Li M, Atmaca-Sonmez P, Othman M, et al. *CFH* haplotypes without the Y402H coding variant show strong association with susceptibility to age-related macular degeneration. Nat Genet 2006;38:1049–54.
18. Maller J, George S, Purcell S, et al. Common variation in three genes, including a noncoding variant in *CFH*, strongly influences risk of age-related macular degeneration. Nat Genet 2006;38:1055–9.
19. Hughes AE, Orr N, Esfandiary H, et al. A common *CFH* haplotype, with deletion of *CFHR1* and *CFHR3*, is associated with lower risk of age-related macular degeneration. Nat Genet 2006;38:1173–7.
20. Coleman HR, Chan CC, Ferris FL III, Chew EY. Age-related macular degeneration. Lancet 2008;372:1835–45.
21. Barrett JC, Hansoul S, Nicolae DL, et al. NIDDK IBD Genetics Consortium, Belgian-French IBD consortium, Wellcome Trust Case Control Consortium. Genome-wide association defines more than 30 distinct susceptibility loci for Crohn's disease. Nat Genet 2008;40:955–62.
22. Sirota M, Schaub MA, Batzoglou S, et al. Autoimmune disease classification by inverse association with SNP alleles. PLoS Genet [serial online] 2009;5:e1000792. Available at: http://www.plosgenetics.org/article/info%3Adoi%2F10.1371%2Fjournal.pgen.1000792. Accessed October 30, 2013.
23. Gregersen PK, Amos CI, Lee AT, et al. *REL*, encoding a member of the NF-kappaB family of transcription factors, is a newly defined risk locus for rheumatoid arthritis. Nat Genet 2009;41:820–3.
24. Bowes J, Ho P, Flynn E, et al. Comprehensive assessment of rheumatoid arthritis susceptibility loci in a large psoriatic arthritis cohort. Ann Rheum Dis 2012;71:1350–4.
25. Gharavi AG, Kiryluk K, Choi M, et al. Genome-wide association study identifies susceptibility loci for IgA nephropathy. Nat Genet 2011;43:321–7.
26. Wright AF. A rare variant in *CFH* directly links age-related macular degeneration with rare glomerular nephropathies. Nat Genet 2011;43:1176–7.

Footnotes and Financial Disclosures

Originally received: June 12, 2013.
Final revision: November 6, 2013.
Accepted: November 6, 2013.
Available online: December 23, 2013. Manuscript no. 2013-939.

[1] Department of Surgery, Division of Ophthalmology, Kobe University Graduate School of Medicine, Kobe, Japan.

[2] Medical Corporation Ryokuwakai Kondo Ophthalmic Clinic, Akashi, Japan.

Financial Disclosure(s):
The author(s) have no proprietary or commercial interest in any materials discussed in this article.

Supported by the Ministry of Education, Science, and Culture, Tokyo, Japan (Grant-in-Aid [B] 24791856). The funding organization had no role in the design or conduct of this research.

Correspondence:
Naoshi Kondo, MD, PhD, Medical Corporation Ryokuwakai Kondo Ophthalmic Clinic, 1-3-7 Ekimae, Ookubo-cho, Akashi 674-0058, Japan.
E-mail: nskondo@gmail.com.

Review

Ophthalmologica

Ophthalmologica 2014;231:59–74
DOI: 10.1159/000355488

Received: August 28, 2013
Accepted: September 1, 2013
Published online: November 21, 2013

Polypoidal Choroidal Vasculopathy: Clinical Features and Genetic Predisposition

Shigeru Honda Wataru Matsumiya Akira Negi

Division of Ophthalmology, Department of Surgery, Kobe University Graduate School of Medicine, Kobe, Japan

Key Words
Polypoidal choroidal vasculopathy · Choroidal neovascularization · Clinical features · Genetic predisposition

Abstract
Polypoidal choroidal vasculopathy (PCV) is currently recognized as a phenotype of age-related macular degeneration (AMD). PCV is believed to be a type of choroidal neovascularization, although some cases of PCV show a distinct vascular abnormality of the choroidal vessels. PCV often shows several unique clinical manifestations which are apparently different from typical neovascular AMD (tAMD). In addition, the natural course and response to treatment are often different between tAMD and PCV. Moreover, recent genetic studies suggested a possible difference in the genetic susceptibility to disease between tAMD and PCV, as well as the existence of heterogeneity among PCV cases. In viewing the accumulation of knowledge about PCV, we have summarized the recent literature regarding PCV in this review article to improve the understanding of this clinical entity including possible susceptibility genes. We will also discuss the optimal treatment strategies for PCV in accordance with the results of recent clinical and genetic studies.

Introduction

Polypoidal choroidal vasculopathy (PCV) was first described in the early 1980s and was originally thought to be a distinct abnormality of the choroidal vasculature found in the peripapillary area [1–3]. However, subsequent reports showed a broad clinical spectrum of PCV, and some authors suggested that PCV is a type of choroidal neovascularization (CNV) [4–6]. Hence, PCV is currently categorized as a phenotype of age-related macular degeneration (AMD), and most ophthalmologists believe that PCV is a type of CNV caused by AMD, although some reports suggested that some cases of PCV are indeed a distinct vascular abnormality of the choroidal vessels. PCV often shows several unique clinical manifestations which are apparently different from typical neovascular AMD (tAMD). For example, distinct polypoidal lesions are the most characteristic feature of PCV (fig. 1). PCV is often found in the extramacular area, whereas tAMD always exists within the macular area [7, 8]. In addition, the natural course and response to treatment are often different between tAMD and PCV [9–17]. Moreover, recent genetic studies suggested a possible difference in the genetic background between tAMD and PCV [18–25], as well as the existence of heterogeneity among PCV cases [26, 27]. Considering the accumulated knowledge about PCV, we now have to reconsider the rationale for understanding and treating this clinical entity. In this

KARGER

E-Mail karger@karger.com
www.karger.com/oph

0030–3755/13/2312–0059$38.00/0

Shigeru Honda, MD, PhD
Division of Ophthalmology, Department of Surgery
Kobe University Graduate School of Medicine
7-5-2 Kusunoki-cho, Chuo-ku, Kobe 650-0017 (Japan)
E-Mail sighonda@med.kobe-u.ac.jp

Color version available online

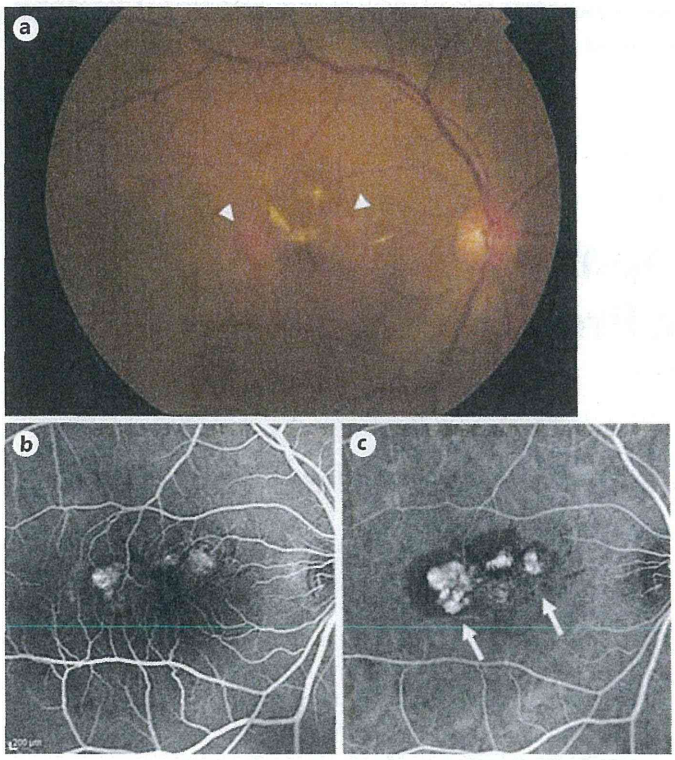

Fig. 1. Fundus photography, fluorescein angiography and indocyanine green angiography images of PCV. **a** Orange-red lesions (arrowheads) are found at the posterior pole of the retina. **b** Dye leakage occurred from the lesions in fluorescein angiography. **c** Distinct polypoidal lesions (arrows) are found in indocyanine green angiography.

review article, the recent literature regarding PCV is first summarized to understand the clinical presentation of PCV, which can be divided into: (1) the common features between PCV and tAMD, and (2) some unique characteristics that are considered specific for PCV. Second, the possible genetic factors responsible for the phenotypes of PCV are introduced. Third, the optimal treatment strategies for PCV are discussed.

Epidemiology

The age range of the patients in previous reports [13, 28, 29] was 21–93 years, and the mean was 68.4 years. PCV is more prevalent in Asian and African-American populations than Caucasians, which may cause the heterogeneity in the clinical features of AMD among the races. Previous studies reported that PCV accounts for 23.0–54.7% of patients with neovascular AMD in the Japanese [11, 20, 30], 49% in the Taiwanese [31], 22.3–24.5% in the Chinese [32, 33] and 22.2–24.6% in the Korean populations [34, 35], but in only about 8–13% of Caucasians [36]. African-Americans are also known to be susceptible to PCV, although no epidemiological study for black people has been reported to date. PCV is more prevalent in men than women in Asian populations (22–37% female), but the opposite is observed in Caucasians (52–65% female) [28]. It is also reported that PCV often affects African-American women. Bilateral cases were reported in 9–18% of Asians (Japanese) and 21–55% of Caucasians. The majority of PCVs (62–94%) are located in the macular area in Asian cohorts, but peripapillary PCV (fig. 2) was frequently observed (18–75%) in American and European cohorts [28]. Moreover, PCV can be located outside the posterior vascular arcade, which may cause peripheral exudative hemorrhagic chorioretinopathy [7, 8]. In some PCV cases, a lesion beneath the macula and remote lesions are found simultaneously [37]. It is unknown why such ethnic variation exists in the epidemiology of PCV. Recent genetic studies suggested that some genetic factors may be associated with the clinical feature of PCV, which could be the reason for such ethnic variations in PCV.Several studies have determined the systemic and ocular risk factors of PCV. They reported that 41–45% of PCV patients had systemic hypertension [38–40]. Another report demonstrated that C-reactive protein levels were increased in patients with PCV [41]. Cigarette smoking is a potent risk factor for PCV [42], and a history of central serous chorioretinopathy was a significant risk factor for PCV [38].

Clinical Manifestation

In accordance with the literature, PCV is characterized by: (1) orange-red colored protrusions at the posterior pole of the retina (or sometimes at the peripheral retina), and/or (2) polypoidal lesions found by indocyanine green angiography (ICGA; fig. 1). However, polypoidal lesions may not be found due to hemorrhage blockage or insufficient image quality in some cases, which makes the diagnosis of PCV difficult. Such cases may be classified as 'suspected of PCV' [43], but it is often very difficult to distinguish those cases from tAMD.

The PCV lesions usually appear as reddish or nonreddish pigment epithelial detachments (PEDs) and are occasionally accompanied by serous retinal detachment (SRD), subretinal hemorrhage, subretinal fibrinous material, hard exudates and drusens. The funduscopic find-

Color version available online

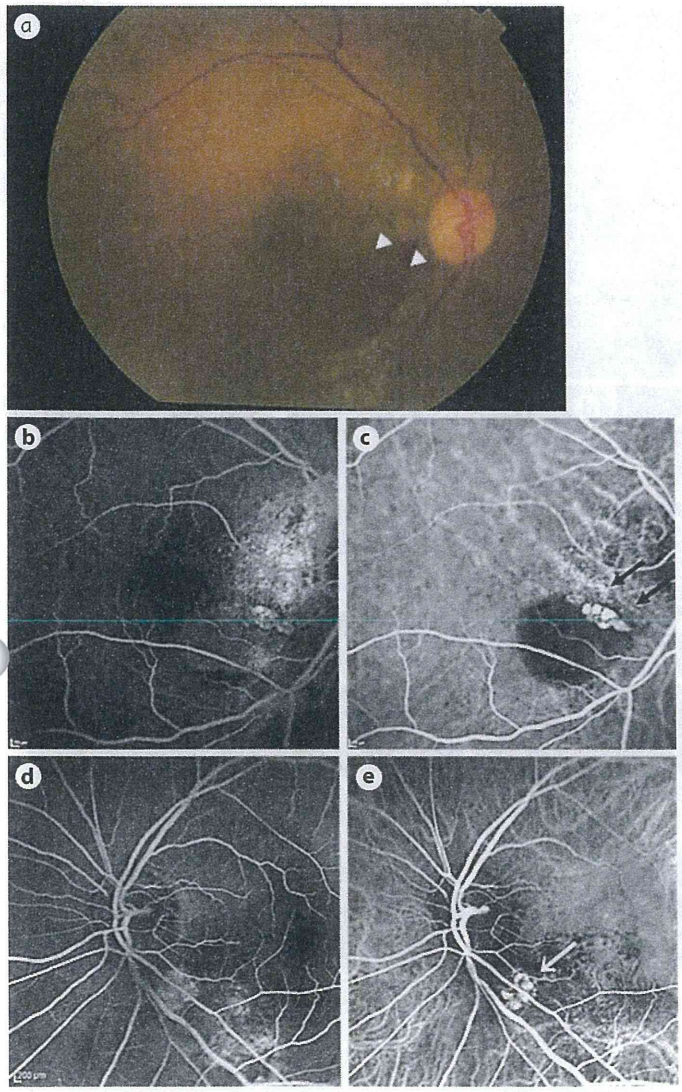

Fig. 2. Fundus photography, fluorescein angiography and indocyanine green angiography images of peripapillary PCV. **a** Orange-red lesions (arrowheads) at the margin and inside serous PED are found in the peripapillary area. **b** Window defect and staining of retinal pigment epithelium are found by the optic nerve head in fluorescein angiography. Note that the fovea is not involved. **c** A cluster of polypoidal lesions (black arrows) is found in indocyanine green angiography. **d**, **e** Another case of peripapillary PCV. Clustered polypoidal lesions (white arrow) are found at the lower position of the optic nerve head.

ings at the initial visit may vary depending on when the patients visit the hospital. Although Uyama et al. [12] reported that about 83% (10 out of 12 cases) of PCV patients showed SRD at the first visit, Sho et al. [11] reported that about 52% of PCV patients showed SRD. In a recent report, Bessho et al. [13] observed SRD in 91% of the patients, and subretinal hemorrhage in 62% of the patients with PCV at the first examination. Previous studies have reported that polyp lesions are mostly present at the margin and inside the serosanguinous PED, which may present as a 'notch sign' between the PED, including polyp lesions and connecting PED, which includes abnormal network vessels [11]. Two previous studies also reported that subretinal fibrinous material on the PED is often observed in PCV [44, 45]. Retinal pigment epithelium (RPE) abnormalities (i.e. hyperplasia, atrophy) are frequently found overlying and around the lesions [11, 13]. Microrips of the RPE and RPE tears could be found at the margins of the PEDs [46, 47]. In some cases, multiple PEDs may span widely at the posterior pole of the retina, or more than 2 independent lesions could be found (i.e. one lesion at the macula and the other at the nasal retina) [48]. However, unlike tAMD, cases with no exudative changes are relatively common in PCV.

The visual acuity (VA) at the initial visit may vary depending on the degree of the exudative change. Those cases without subretinal hemorrhage and with no or slight SRD have good VA, whereas VA in those cases with severe exudative changes may be affected. However, the mean VA in PCV patients was generally better than in tAMD at baseline [49]. This is likely because PCV lesions remain under the RPE in the early stages, while tAMD occasionally develops CNV in the subretinal space (the so-called type 2 CNV), which may affect the sensory retina directly.

Angiographic Imaging

Unfortunately, fluorescein angiography (FA) is not an optimal tool to make a diagnosis of PCV, since FA is not sufficient to visualize the structures in the inner choroidal space where PCV likely exists. However, a 'window defect' reflecting RPE atrophy is often observed, and the underlying polypoidal lesions may be found as 'hyperfluorescent spots' by FA in certain PCV cases [28]. Subretinal fibrinous material, if it exists, can be observed as an expanding fluorescent leakage that may simulate the classic lesion of tAMD found by FA [44, 45]. This appearance might be termed a 'pseudoclassic CNV lesion', which is a characteristic of PCV (fig. 3).

In ICGA, PCV is typically characterized by distinct forms of choroidal vascular abnormalities, including characteristic polypoidal lesions with or without branching vascular networks (BVNs) of choroidal origin [50]. As described above, polyp lesions are mostly present at the mar-

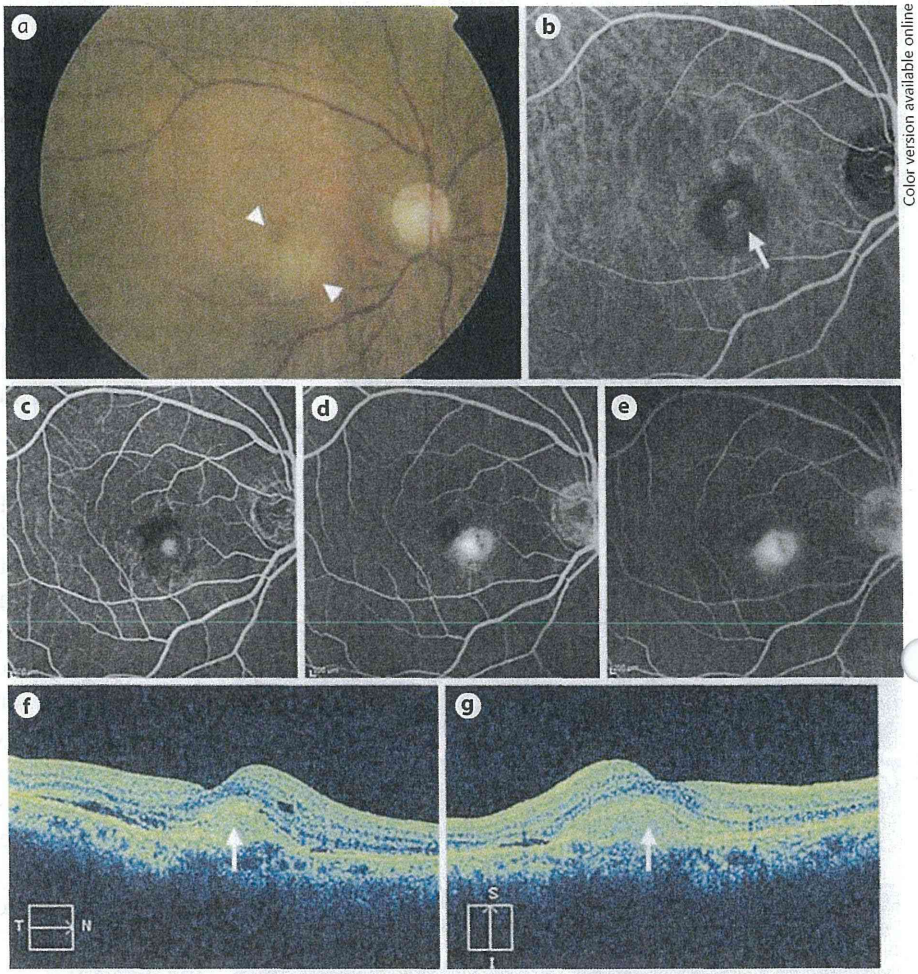

Color version available online

Fig. 3. Fundus photography, FA, ICGA and optical coherence tomography images of PCV which simulates tAMD. **a** A fibrinous subfoveal lesion (arrowheads) with subretinal hemorrhage is found in the juxtafoveal region. **b** A solitary polyp lesion (arrow) is found in ICGA. **c–e** A presentation similar to predominantly classic CNV is found in FA, although there is no true classic lesion. **c–e** represent the image at 1, 5 and 10 min, respectively. This manifestation could be called 'pseudoclassic CNV appearance'. **f, g** Subretinal fibrinous material (arrows) occupying the subretinal space is found by optical coherence tomography.

gin and inside the PED, which may cause a 'notch sign' between the PED, including polyp lesions and connecting PED, which includes the BVN. Clustered grape-like polypoidal lesions on ICGA were observed frequently (25–67%) in Asian populations [12, 13, 48]. It is very unique for PCV that some cases show pulsations of the polypoidal lesions in the early phase of ICGA [50–52]. Dilatation of choroidal vessels found in the early and middle phases of ICGA is another unique feature of PCV (fig. 4). Choroidal vascular hyperpermeability is often found in PCV by ICGA in the late phases, and is likely due to the staining of fibrinous materials which exist around the dilated choroidal vessels [53–55]. PCV cases show wide variation in their size, and the features of the BVN and polypoidal lesions. The Japanese Study Group of Polypoidal Choroidal Vasculopathy proposed that PCV with only BVN and no apparent polypoidal lesions may exist, and those cases are termed 'suspected of PCV' [43]. However, those cases are often difficult to distinguish from tAMD. The variations of PCV in its presentation may be only due to the stage of the disease (more progressed disease should have larger lesions) [56], but evidence is accumulating which supports the existence of subtypes in PCV.

Recent studies have described the subclassification of PCV regarding the presence or absence of BVN (as feeder vessels for the polyp lesions) found by ICGA [57–59]. Thus, PCV with apparent BVN is called 'type 1 PCV' or 'polypoidal CNV', whereas the one with no or only faint BVN is called 'type 2 PCV' or 'typical PCV' (fig. 5). The presence or absence of BVN can usually be determined within 1 min starting from the injection of ICGA, but some cases are difficult to classify. Recent studies demonstrated that these 2 angiographic subtypes of PCV showed differences in their clinical course, genetic susceptibility and response to therapy. Type 1 PCV usually has larger lesion sizes due to the larger and more distinct BVN,